


A Non-Invasive Methodology for Magnetic Characterization of Transformers and Reactors

Jônatas P. Américo¹, Jean V. Leite², Cristian F. Mazzola²,

¹ Department of Electrical Engineering, Federal University of Technology – Paraná, Pato Branco 85503-390, Brazil, jonatasamerico@utfpr.edu.br

² Department of Electrical and Electronic Engineering, Federal University of Santa Catarina, Florianópolis 88040-900, Brazil, jean.vianei@ufsc.br; cristian@eel.ufsc.br

Abstract— The lack of data is a hindrance to the experimental determination of magnetic cores characteristics. This work presents a non-invasive and field-applicable methodology for electromagnetic devices characterization. Based on fundamental equations of electromagnetism and routine tests, the methodology was applied to obtain, at low frequency: the core loss separation, the hysteresis loop and its BH curve of a three-phase dry core-type transformer. The required equipment and the procedures to do the characterization are presented and discussed. The results were compared with experimental data obtained from tests that were carried out on the same material using a Single Sheet Tester device. The results show a difference in losses of 4.9% for hysteresis, 1.5% for dynamic, and 3.3% for total losses. In the no-load test comparison there was a difference of 4% for dynamics and 1.8% in total losses. The proposed methodology can be applied to different magnetic core types as well as to single-phase transformers and reactors.

Index Terms— Electric transformer, hysteresis loop, magnetic characterization, magnetic losses, magnetic materials, transformer core loss, transformer testing.

I. INTRODUCTION

Electromagnetic devices are important pieces of equipment in electrical systems, being their performance crucial for their operation [1], [2]. It is commonly necessary to model such equipment to analyze its performance in the most varied electrical regimes in which the system can operate as, for instance, the transient regime. The accuracy of their modeling is strongly dependent on the nonlinear behavior of the ferromagnetic core [3]. The core characterization of devices onsite can be a challenge due to the lack of its electric and magnetic data and the complexity of representing the nonlinear behavior of the magnetic core [4]–[6]. This fact may require simplifications that sometimes can cause significant deviations from the expected precision for representing such devices.

In studies on ferroresonance phenomena, for example, due to the unavailability of data, the transformer core is usually represented by a single-valued magnetizing inductance combined to a resistance representing the total core loss [4]. However, this resistance does not have a constant value and decreases as the core excitation level increases [7]. Other studies discuss the use of the parallel combination of a nonlinear resistance and an inductance, which is determined from tests at different excitation levels. This approach has limitations since the hysteresis loss depends on the maximum flux level and not on the maximum voltage level [8]. More realistic representations must include the effects of magnetic hysteresis and eddy currents [8]–[10]. If the effect of hysteresis is neglected in the ferroresonance

analysis, a lower accuracy in the determination of the magnetization characteristics, core loss and waveforms will be achieved [4], [7], [11].

For inrush current analysis, a simplified approach such as linear magnetization in two segments is often used. However, when there is a remanent magnetization in the ferromagnetic core, disregarding the magnetic hysteresis affects the dynamic and magnitude of the inrush current [12]–[15]. Another example in electrical power systems is the devices modeling for short-circuits calculus. In such problems, the magnetic characteristics of three-phase transformers and grounding reactors are usually required.

Several works have proposed magnetic material models in order to represent ferromagnetic cores. The analysis of core losses in single-phase and three-phase transformers was presented, respectively, in [16] and [17]. The equivalent magnetic core circuit, represented by a hysteresis locus, was applied to calculate the differential permeability in the model [16]. In [18], a modeling based on the duality between the electric and magnetic circuit was proposed for three-phase transformers with asymmetrical cores, being the magnetic hysteresis used to represent each core section. In [4], Preisach's hysteresis model was proposed for ferroresonance analysis. In [19], the inrush current was represented by a nonlinear resistance that varies instantaneously with the magnetization flux.

In each of the studies mentioned above, it was necessary to model the magnetic circuit of the device under analysis. However, this process can be challenging if there is a lack of data, for instance, when the electric steel characteristics are unknown and there is no access to sophisticated equipment for material characterization tests [20], [21]. In addition, occasionally, it is necessary to model devices in operation, where the characteristics of its electric steel sheets may vary due to thermal stress, steel sheets aging [22] or even because of mechanical stress during its assembly or transport.

The main contribution of this work is to propose a methodology for experimental characterization of magnetic devices without the need of previous tests in laboratory or invasive procedures in the core structure or in the windings. This study presents: description and details of the tests that must be carried out; a case study; and the measuring instruments used. Combined with a loss model, the methodology proposed allows to obtain the BH loop of the core at low frequency, as well as a separation of the magnetic losses. The technique was applied to a 2 kVA three-phase dry-type transformer and the results were compared with the reference data obtained from tests that were carried out on the same material using a Single Sheet Tester (SST) device.

The following section reviews the equations for the calculation of losses in ferromagnetic materials applicable to transformers and reactors. This can be useful to understand the experimental procedures and modeling that is presented next.

II. CALCULATION OF THE LOSSES IN THE MAGNETIC CORE OF TRANSFORMERS

No-load losses or core losses occur when transformers are excited at rated voltage, but no loads are connected to the secondary winding. In this case, the total flux is present in the magnetic core and only the magnetizing current flux is present in the primary windings. The total core losses can be separated into hysteresis losses W_h , eddy current losses W_f , and excess losses W_e [23]–[25].

When some ferromagnetic material is subjected to a time-varying periodic magnetic field H with frequency f , there will be a hysteresis loop (BH curve at low frequency). The loss due to the magnetic hysteresis, W_h , per unit of mass, in a period T , is defined by (1), where m_v is the material specific

mass.

$$W_h = \frac{1}{m_v} \int_{B|_{t=0}}^{B|_{t=T}} H dB \quad (1)$$

Equation (2) defines W_f for rectangular section electrical steel sheets. W_f is due to eddy currents in the core when it is under a time-varying flux regime. This effect creates rings of currents perpendicular to the direction of the induction circulation in the steel sheets [26].

$$W_f = \frac{\sigma \cdot d^2}{12 \cdot f \cdot m_v} \frac{1}{T} \int_0^T \left(\frac{\partial B}{\partial t} \right)^2 dt, \quad (2)$$

where σ , d and B are, respectively, the electrical conductivity of the sheets, the thickness of the sheets, and the magnetic induction.

When the energy balance is performed, values higher than those classically obtained by hysteresis and eddy currents are noticed. The losses estimated through classical separation between hysteresis and eddy currents are lower than the total losses measured and this difference is called excess magnetic loss W_e . The average value of W_e , per period and unit of mass, is determined by (3) [27].

$$W_e = \frac{1}{f \cdot m_v} \sqrt{\sigma G V_o S} \frac{1}{T} \int_0^T \left| \frac{dB(t)}{dt} \right|^{\frac{3}{2}} dt, \quad (3)$$

where σ , G , V_o , and S are, respectively, the electrical conductivity of the sheets, a dimensionless coefficient that represents the coefficient of friction of magnetic object, the equivalent of a coercive field of the magnetic object, and the cross-sectional area of the lamination [28]. However, the coefficient $\sqrt{\sigma G V_o S}$ is usually assumed to be a constant that depends on the material.

The total core losses W_t , in a magnetic sheet submitted to a periodic alternating magnetic induction is given by the sum of W_h , W_f , and W_e .

III. PROCEDURES FOR THE CHARACTERIZATION OF THE MAGNETIC CORE

For the characterization of the core, a Reduced Frequency Test (RFT) and the classical, open-circuit and short-circuit tests, are necessary. Such tests allow knowing the characteristics of core saturation, hysteresis losses, other losses of magnetic origin and the losses in the windings.

The methodology proposed is based on fundamental equations of electromagnetism and routine tests performed on electrical transformers. The procedure is described as follows, indicating the necessary voltage sources and measuring instruments, how the number of winding turns is carried out, the determination of the magnetic parameters of the core, and the conduction of the reduced frequency test and additional tests.

A. Equipment and instruments required

The equipment required is:

- A power supply that allows the control of the applied frequency and the imposition of the device rated current and voltage;
- Instruments for voltage, current, and power measurements;
- Equipment for the acquisition of voltage and current waveforms and its respective probes;
- Voltage and current transformers to adjust the amplitudes of the acquired signals (if necessary).

It is noteworthy that the voltage source with variable frequency is the most unusual device among those listed. The source must be controlled to maintain the symmetry of the waveforms. A synchronous generator can be used as the power source, controlling the frequency of the terminal voltage by the speed of the primary machine.

B. Determination of winding turns

If the number of winding turns is unknown or if there is any doubt about its real value, this quantity can be determined experimentally by building auxiliary windings above the original transformer windings. By applying a voltage in the winding under analysis, at the rated operating frequency, and measuring the induced voltage in the auxiliary winding, the number of winding turns can be obtained from the transformation ratio. The auxiliary winding should be placed in the center of the winding under analysis to avoid distortions in the magnetic flux from the winding heads. It is recommended to do several voltage measurements, starting from a low voltage level, increasing it up to the rated voltage. The auxiliary windings should fill at least 25% of the height of the windings under analysis, which can be extended up to 50%.

C. Core dimensions and mean magnetic path length

It is necessary to determine the core mean magnetic path length l_{eq} . If the device design is not available, measurements of the core structure are necessary. However, if the core is encapsulated or immersed in an oil tank, the determination of the mean magnetic path can only be done with the geometric data provided by the device manufacturer. A careful analysis of the magnetic circuit must be carried out, determining the more relevant path of the field from the excited winding. This determination depends on the type of the transformer core and the choice of the windings in which the RFT is performed. Fig. 1 shows some different types of transformer cores, evidencing that the determination of the mean magnetic path lengths must be done with criteria.

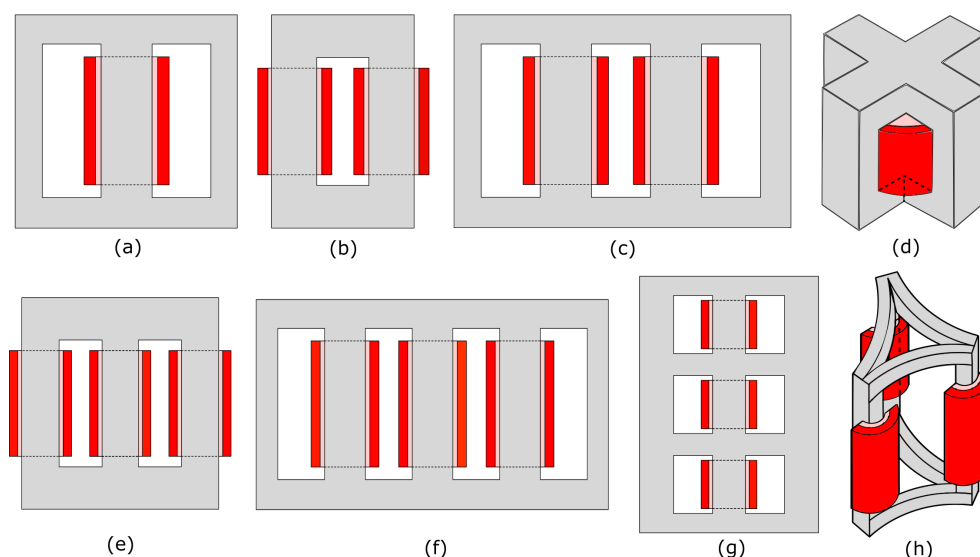


Fig. 1. Different types of magnetic core. (a - d) Single-phase transformers. (e - h) Three-phase transformers.

l_{eq} can be seen as an average magnetic path equivalent to the parallel combination of the magnetic reluctances of the core. At this point, for square section and stepped magnetic cores, the following

steps must be accomplished:

- 1) To determine the cross-sections and the magnetic field circulation paths, the dimensions of the magnetic core yokes and legs must be measured;
- 2) The winding where the RFT is performed must be selected and the mean magnetic path length is estimated using the core dimensions.

D. Conducting the test at reduced frequency

A voltage at reduced frequency must be applied and the current measured in the selected primary winding. The induced voltage in the secondary winding, in the same leg, must be measured. This voltage value is used to calculate the magnetic induction. The choice of secondary winding allows the determination of the magnetic induction without having to determine the voltage drop in the series parameters due to the magnetizing current. In addition, it is desirable to measure peak and RMS values of the voltages and currents for observation and treatment of the experimental data.

If it is possible to examine the flux-current loop during the test, it should be verified if the magnetic induction is in the non-linear region (above the BH loop "knee") for the saturation characterization. When this is not possible, the non-linearity should be observed by examining the measured primary current (see i_p in Fig. 5).

The voltage at reduced frequency is applied because the hysteresis loss is independent of the frequency and the dynamic losses can be disregarded when the frequency is close to zero. Therefore, hysteresis loss is aimed to be obtained at the lowest possible frequency [27]. From previous works, the test is recommended to be performed with a frequency under 5 Hz. As inductive reactances are reduced due to low frequency, a small portion of the rated voltage is required to impose inductions close to saturation. The primary voltage must be increased gradually from zero, observing the primary current so that it does not exceed the rated value.

From an approximation of Ampere's theorem, the magnetic field $H(t)$ can be determined by

$$H(t) = \frac{N_p \cdot i_p(t)}{l_{eq}}, \quad (4)$$

where N_p is the number of turns of the primary winding, $i_p(t)$ is the measured current and l_{eq} is the mean magnetic path length for the selected winding.

The secondary voltage $v_s(t)$ is related to the variation of the flux ϕ with respect to time, by

$$v_s(t) = N_s \cdot \frac{d\phi}{dt}, \quad (5)$$

where N_s is the number of turns of the secondary winding. Equation (5) can be approximated written in terms of the magnetic induction $B(t)$, as

$$v_s(t) = N_s \cdot S \cdot \frac{dB(t)}{dt}, \quad (6)$$

where S represents the cross-sectional area of the magnetic core leg. $B(t)$ is so determined by the integration of $v_s(t)$ with respect to time.

$$B(t) = \frac{1}{N_s \cdot S} \int v_s(t) dt \quad (7)$$

Equation (7) can be solved numerically by using (8), where m is the number of points of the acquired

signal, V is the waveform to be integrated, Δt is the time step and $i = 0, 1, 2, \dots, m - 1$ [27]. When using (8), it must be ensured that the waveform to be integrated starts at the maximum value of the positive voltage semicycle. Otherwise, a continuous level will be incorporated into the signal.

$$\int v(t)dt = \frac{1}{6} \sum_{j=0}^i (V_{j-1} + 4V_j + V_{j+1}) \Delta t \quad (8)$$

Special attention must be paid to this test, because a slight increase in the applied voltage can already cause the saturation of the magnetic core, which would, consequently, cause an exponential current increase. The voltage required to obtain the core saturation will depend on the test frequency. During the test, it must be guaranteed that the current does not exceed the winding rated limits.

From the reduced frequency test, one can obtain the hysteresis loop, and consequently, the hysteresis core loss per unit of volume, in J/m^3 . This data allows estimating the hysteresis losses in the entire core volume. Additionally, the BH loop allows the representation of core magnetic saturation.

E. Open-circuit and short-circuit tests

The measurement of total core losses, at rated frequency, can be achieved by the no-load (open-circuit) test [29]. The test consists in exciting the lower voltage winding with rated voltage, keeping the other one unloaded, and then measuring the active power [30], [31].

The series parameters of each winding can be determined by the short-circuit test. It consists of applying a voltage to achieve the rated current in the higher voltage winding while the other one is short-circuited [8]. The parameters are calculated by:

$$R_p = \alpha \cdot \frac{P_{sc}}{I_{sc}^2}, \quad (9)$$

$$R_s = \frac{1 - \alpha}{n^2} \cdot \frac{P_{sc}}{I_{sc}^2}, \quad (10)$$

$$X_p = \alpha \cdot \sqrt{\left(\frac{V_{sc}}{I_{sc}}\right)^2 - \left(\frac{P_{sc}}{I_{sc}^2}\right)^2}, \quad (11)$$

$$X_s = \frac{1 - \alpha}{n^2} \cdot \sqrt{\left(\frac{V_{sc}}{I_{sc}}\right)^2 - \left(\frac{P_{sc}}{I_{sc}^2}\right)^2}, \quad (12)$$

where P_{sc} is the three-phase active short-circuit power, I_{sc} is the phase short-circuit current, V_{sc} is the phase short-circuit voltage, n is the transformation ratio and α relates the parameter distribution between the primary and secondary windings. From the open-circuit test, the total core losses are obtained. The dynamic losses are so obtained by subtracting the hysteresis loss from the total core losses.

The procedure presented above allows the obtaining of the BH loop at low frequency as well as the hysteresis and dynamic losses of the core. From the BH loop, it is possible to obtain the magnetic permeability of steel for most different types of modeling. Short-circuit and open-circuit tests also allow obtaining winding resistances and leakage reactances. This combined data allows the core modeling for different device operating regimes.

For a better understanding of the proposed methodology a step-by-step and a flowchart (Fig. 2) are presented as follows:

- 1) Determination of winding turns;
 - a) If the number of winding turns is unknown, auxiliary windings must be built above the original transformer windings and N_p and N_s must be determined according to Section III-B;
- 2) Magnetic core dimensions;
 - a) If the core design is not available, the core dimensions should be measured as shown in Fig. 4;
- 3) Determination of mean magnetic path length;
 - a) Identify the type of magnetic core construction (see Fig. 1) and choose the winding (Win_p) in which the reduced frequency test (RFT) is performed;
 - b) Determine, based on item 3a, the mean magnetic path length (l_{eq});
- 4) Reduced frequency test;
 - a) Connect the variable frequency voltage source to the chosen winding (Win_p) and the voltage acquisition device to the secondary winding (Win_s) of the same core leg where the reduced frequency voltage is applied, while keeping all the other windings open;
 - b) Apply the voltage at reduced frequency, gradually, to the chosen winding (Win_p), verifying if the magnetic induction is in the non-linear region (above the BH loop "knee"). This test is recommended to be performed with a frequency under 5 Hz;
 - c) Acquire the magnetizing current (i_p) in the winding (Win_p);
 - d) Acquire the induced voltage (v_s) in the secondary winding (Win_s);
 - e) Calculate the magnetic field ($H(t)$) by using (4), considering N_p from item 1, l_{eq} from item 3b and i_p from item 4c;
 - f) Calculate the magnetic induction ($B(t)$) using (7), considering N_s from item 1 and v_s from item 4d. Equation (8) can be used to solve the integral of $v(t)dt$;
- 5) Open-circuit test;
 - a) Supply the lower voltage winding at rated voltage and frequency, keeping the other windings unloaded, and then measure the active power;
- 6) Short-circuit test;
 - a) Supply the primary winding while the secondary is short-circuited. Apply only the voltage needed to reach the rated current;
 - b) Measure voltage (V_{sc}), current (I_{sc}), and active power (P_{sc});
 - c) Calculate the series parameters by using (9), (10), (11) and (12), considering V_{sc} , I_{sc} and P_{sc} from item 6b.

To validate the proposed procedure, a case study was carried out with a commercial transformer that was submitted to the proposed tests. The core steel sheets were characterized in laboratory in order to evaluate the methodology accuracy.

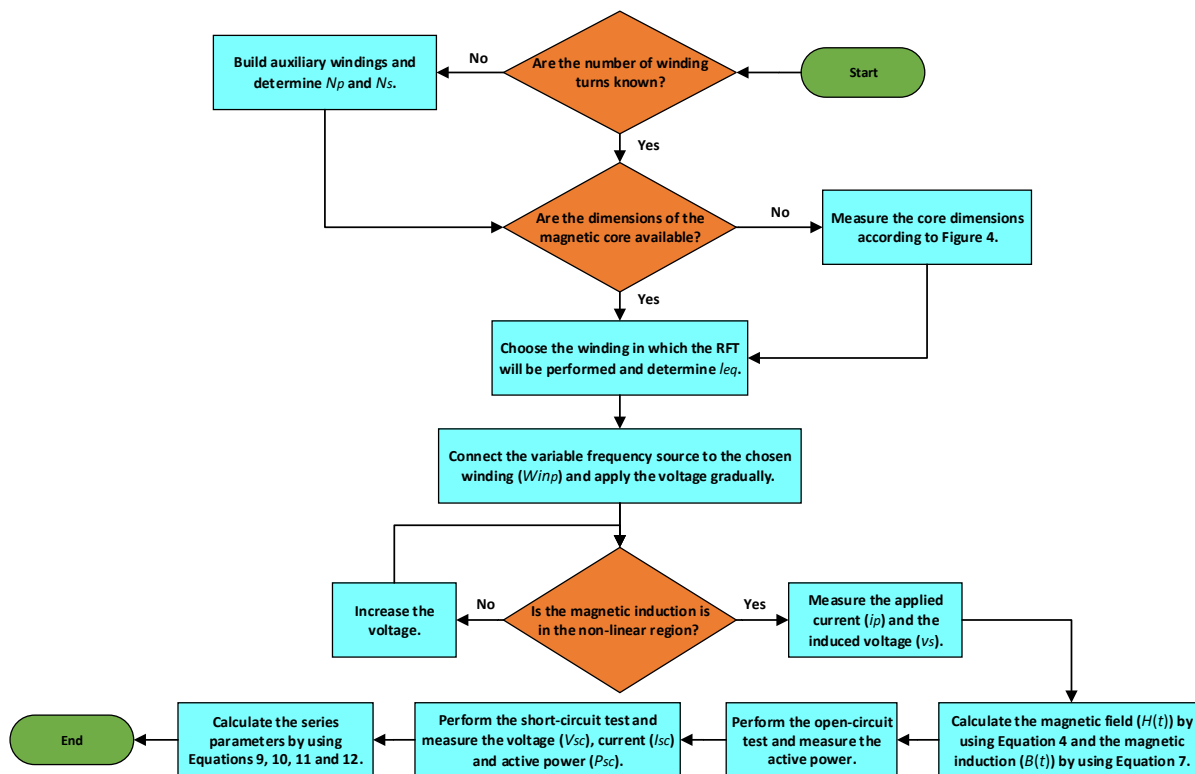


Fig. 2. Flowchart of the proposed methodology.

IV. CASE STUDY

For the case study, the three-phase transformer, illustrated in Fig. 3, was chosen. Its rated data are: 220/127 V; delta-ye connection and power of 2 kVA. The steel sheets used for the manufacturing of this device were available for magnetic characterization in the laboratory. A twin device was also available for additional tests.

The following tests and procedures were performed in order to experimentally characterize the core and validate the results:

- Experimental determination of the number of winding turns;
- Measurement of core dimensions;
- Choice of the windings in which the reduced frequency test is performed and estimation of the mean magnetic path length;
- Reduced frequency test;
- No-load test for the determination of core losses;
- Short-circuit test for determination of the series parameters of the windings.

To validate this methodology, the density and conductivity of the core sheets were determined in laboratory and the sheets characterization tests were performed in a Single Sheet Tester device (SST).

A. Testing apparatus

A synchronous generator was used as the power supply for the tests. The frequency variation was obtained by the speed control of the generator. The signals at reduced frequency were acquired with a sampling rate of 5 kS/s, using the Tektronix TCP0030A current probe with an accuracy of 1%, Tektronix P6117 voltage probe, and the Tektronix DPO3034 oscilloscope with an accuracy of 1.5%.



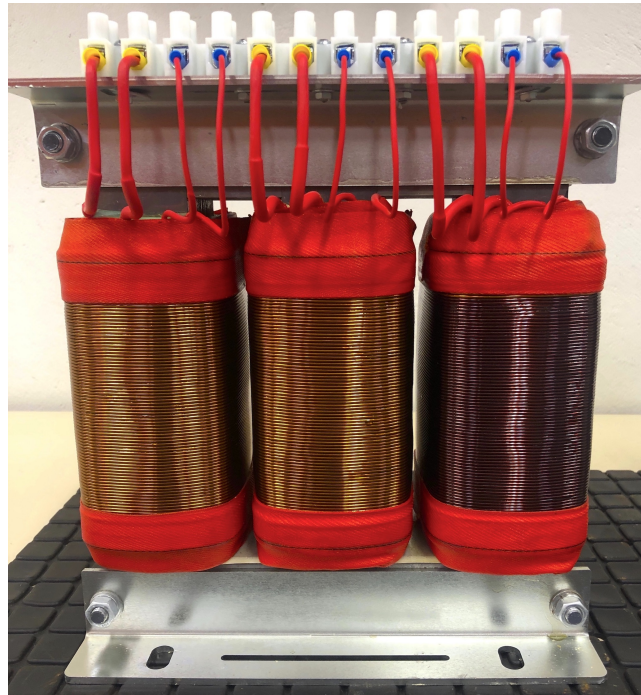


Fig. 3. Three-phase transformer chosen for the case study.

The power, voltage, and current measurements in the open and short-circuit tests were performed with the Yokogawa WT500 power analyzer, with an accuracy of 0.1%. A precision balance with a resolution of 0.01 g was used to determine the density of the sheets. The determination of the conductivity of the sheets were performed by measuring resistance with a four-wire Agilent 34410A Digital Multimeter High Performance device. Validation of the transformer hysteresis loop was performed by testing the core sheets using the Single Sheet Tester of an Electrical Steel Tester MPG 200 Brockhaus. MATLAB software was used to analyze and process the signals.

B. Determination of the number of winding turns, dimensions of the magnetic core and estimation of the mean magnetic path length

The numbers of winding turns were determined by the procedure described in Section III-B. Three auxiliary windings with 20 turns each were built. Voltage is applied to each winding separately and the induced voltage in the auxiliary winding at the same leg is measured. This procedure is carried out for every winding of each transformer's leg. The average results were: $N_p = 288.6$ and $N_s = 96.1$ turns. Comparing these values obtained with those provided by the manufacturer ($N_p = 288$ and $N_s = 96$ turns), a difference of 0.2% for the primary and 0.1% for the secondary winding was obtained.

The windings of the central leg were chosen for the reduced frequency test. Considering this choice, Section III-C, the transformer core dimensions shown in Fig. 4, and $l_{c2} = l_{c3}$, l_{eq} can be determined as

$$l_{eq} = l_{c1} + \frac{(l_{c2} + 2L_p)^2}{2l_{c2} + 4L_p}, \quad (13)$$

where L_p is half the width of the central leg.

Equation (13) is determined for the three-phase transformer of Fig. 1(e), where the RFT is performed on the central leg windings. Depending on the core geometry and the choice of the windings for the

test, l_{eq} changes. Using (13) and the dimensions measured shown in Fig. 4, the l_{eq} was found as $387.5 \cdot 10^{-3}m$. The cross-section area $S = 2.5 \cdot 10^{-3}m^2$ is obtained directly from the measured core dimensions and shown in Fig. 4.

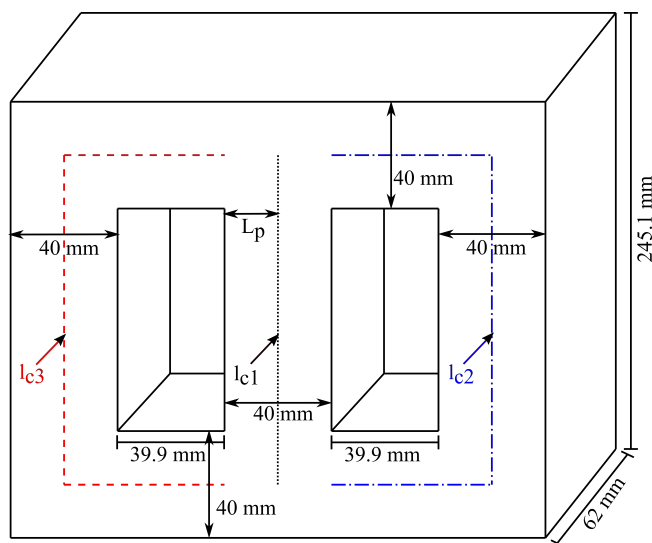


Fig. 4. Transformer core dimensions and mean magnetic paths.

C. Reduced frequency testing

Voltage with reduced frequency is applied to the primary winding of the central leg and its magnetization current is measured. The induced voltage is measured in the secondary winding at the same leg. Fig. 5 shows the measurements at 1.25 Hz, where v_p , v_s and i_p are, respectively, the primary voltage, the secondary voltage and the current in the primary. From Fig. 5 one can see that applying the voltage at reduced frequency, even with the amplitude of 8.6 V peak, the nonlinear characteristic of the core is already observed in the current waveform i_p . Examining the distortion in v_s , when compared to v_p , it can be seen the influence of the voltage drop of the winding series parameters due to the magnetization current.

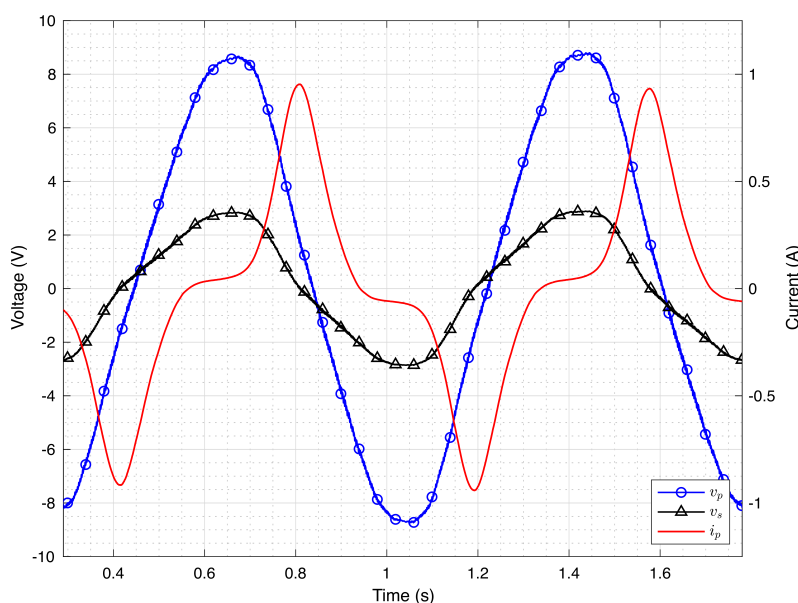


Fig. 5. Transformer test at 1.25 Hz.

Fig. 6 shows the BH loops obtained using (4) and (7) for the frequencies of 1.25, 5, and 10 Hz. As expected, as the test frequency is increased, the area of the BH loop (loss) increases.

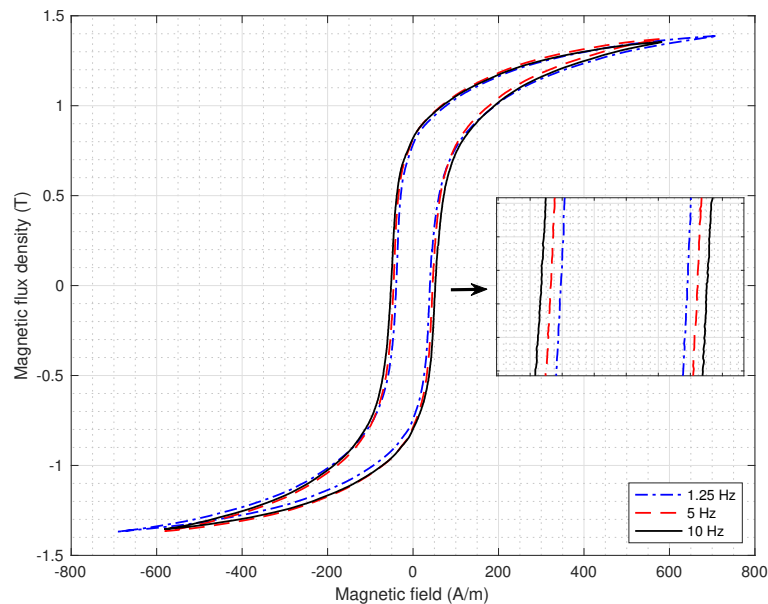


Fig. 6. Experimental BH loops for tests at 1.25 Hz, 5 Hz and 10 Hz.

D. No-load and short-circuit tests

No-load and short-circuit tests are performed after the transformer reaches the steady state temperature, i.e., a variation lower than $1^{\circ}C$ in the last hour of operation [32]. Table I and Table II show, respectively, the average measurements of the no-load and short circuit tests. Using the measurements of Table II and (9), (10), (11), (12) and considering $\alpha = 0.5$ [33], one can obtain $R_p = 1.4 \Omega$, $R_s = 0.1 \Omega$, $L_p = 1.5 \text{ mH}$ and $L_s = 168.4 \mu\text{H}$.

TABLE I. NO-LOAD TEST MEASUREMENTS

| Line voltage (V) | Line current (A) | Three-phase power (W) |
|------------------|------------------|-----------------------|
| 220.5 | 0.5 | 54.0 |

TABLE II. SHORT-CIRCUIT TEST MEASUREMENTS

| Line voltage (V) | Line current (A) | Three-phase power (W) |
|------------------|------------------|-----------------------|
| 9.1 | 5.1 | 75.0 |

V. RESULTS VALIDATION

For results validation, the same steel Sheet Package (SP) used in the transformer was characterized in the laboratory. Initially, to confirm that both are the same material, the RFT was also carried out in a core built with the same dimensions as the transformer under analysis. To perform this test, it was necessary to build windings in the SP (Fig. 7). In each lateral leg, 100 turns were wound. In the central leg, two windings were wound, one with 100 turns and the other with 260 turns. The

primary winding was considered to be the 260 turns one. During the tests, the windings were placed at the center of each leg.

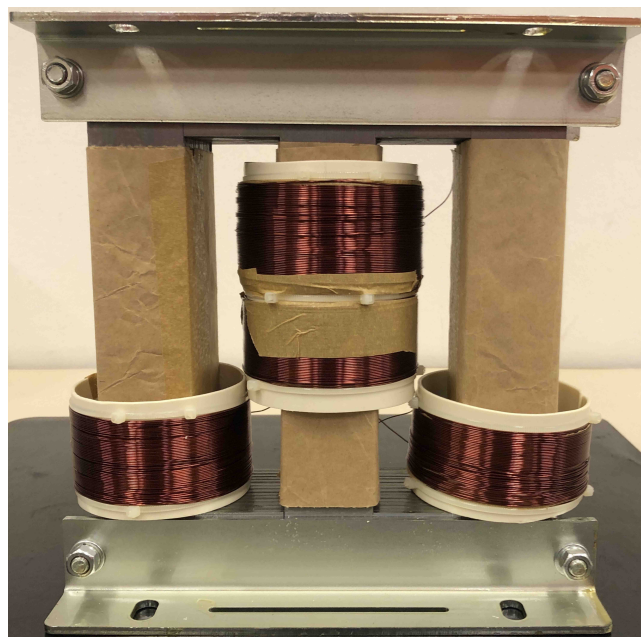


Fig. 7. Sheets Package (SP) and windings built.

Fig. 8 shows the measurements, where i_p is the primary winding current (260 turns) and v_C , v_E and v_D are, respectively, the induced voltages in the windings (100 turns) of the central, left and right legs. Analyzing Fig. 8 one can see the same characteristics of the induced voltage and magnetizing current as seen in Fig. 5. The difference in the induced voltages (v_E and v_D compared to v_C in Fig. 8) is due to the splitting of the flux in the center leg (see Fig. 10). In Fig. 8, unlike in Fig. 5, the voltage applied to the primary winding was not acquired.

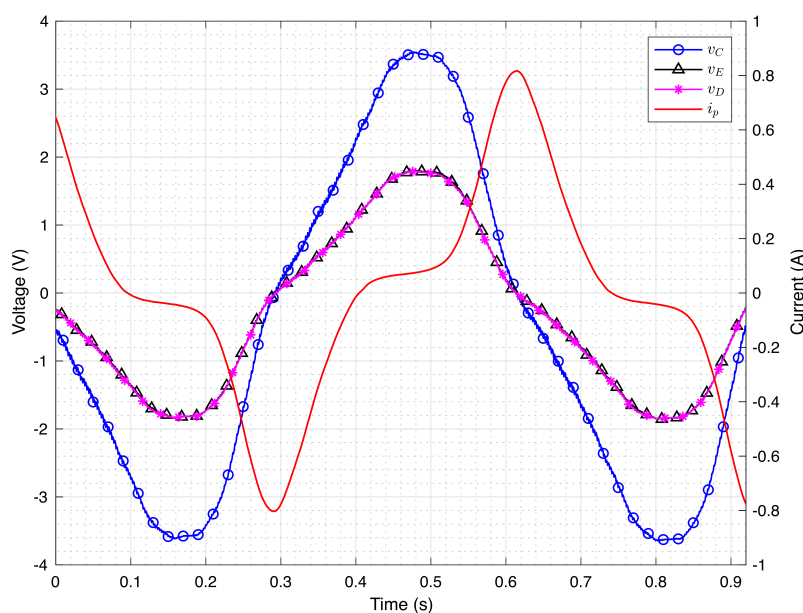


Fig. 8. Test in the SP: current in the central leg winding and induced voltages at all legs windings. The applied voltage is not shown.

Fig. 9 shows the comparison between the BH loops of the transformer and the SP. For the comparison between the BH loops, the energy density was calculated, being 247.9 J/m^3 in the transformer and 243.9 J/m^3 in the SP. The energy density difference between the BH loops calculated is 1.6%. From the results presented, it can be evidenced that both cores were built with the same material.

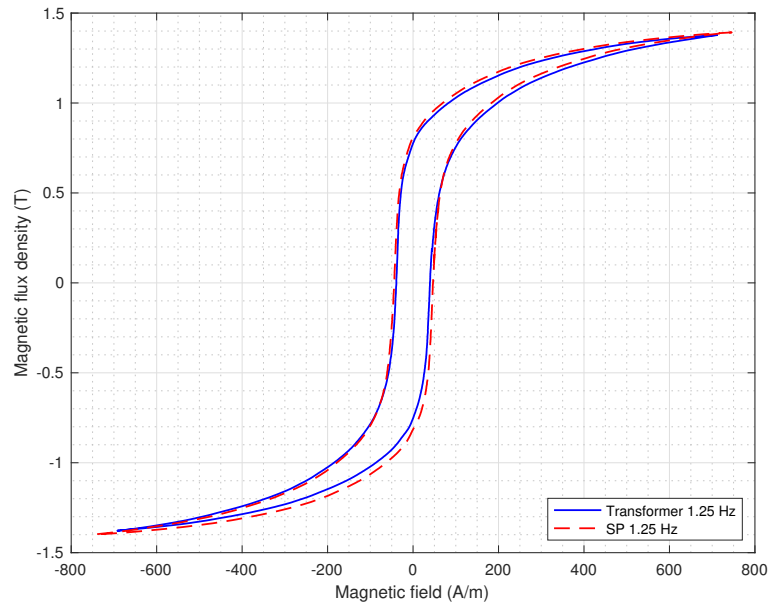


Fig. 9. Comparison between transformer and SP hysteresis loops.

Besides the RFT, an analysis of the magnetic flux was performed, as it is shown in Fig. 10. Where, ϕ_C , ϕ_D , and ϕ_E are, respectively, the fluxes in the center, right, and left legs. For this level of magnetic induction, there is almost no stray flux $\phi_C - (\phi_D + \phi_E)$. This observation is important because it shows that the measured BH loop had no interference of stray fluxes in the core.

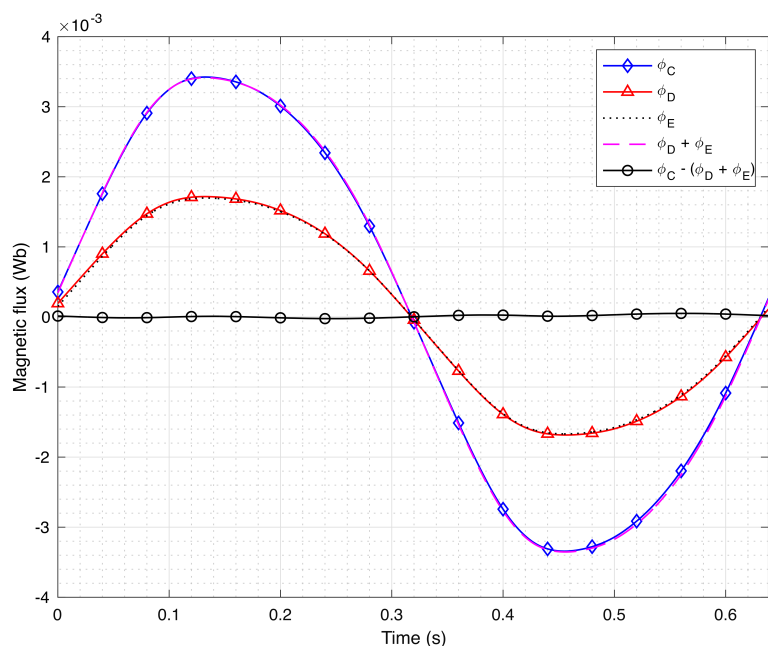


Fig. 10. Magnetic flux in the legs of the SP.

In order to obtain the reference magnetic parameters of the steel sheets for comparison, tests were carried out using a Single Sheet Tester (SST). Three samples were selected for the characterization. Initially, the dimensions and weights of the sheets were obtained and their respective densities calculated, as shown in Table III. From this procedure, an average density of 6876.1 kg/m^3 was found. To validate the density obtained, the procedure described in [34] was applied, in which the density is calculated through the procedure of sheet resistivity measurement. The density obtained with the approach described in the technical standard was 6905.7 kg/m^3 , with a variation of 0.4%.

TABLE III. PARAMETERS OF THE SHEETS USED IN THE SST TEST

| Sheet | Width (m) | Length (m) | Thickness (m) | Weight (kg) | Density (kg/m^3) |
|-------|----------------------|---------------------|---------------------|----------------------|-----------------------------|
| S1 | $30.3 \cdot 10^{-3}$ | | | $25.6 \cdot 10^{-3}$ | 6866.3 |
| S2 | $30.2 \cdot 10^{-3}$ | $205 \cdot 10^{-3}$ | $0.6 \cdot 10^{-3}$ | $25.6 \cdot 10^{-3}$ | 6886.3 |
| S3 | $30.2 \cdot 10^{-3}$ | | | $25.5 \cdot 10^{-3}$ | 6875.6 |

Fig. 11 shows the comparison between the transformer hysteresis loop and the SST for the three sheets analyzed. In the comparison, the experimental data at 5 Hz was used because the SST has an initial analysis frequency of 3 Hz [35].

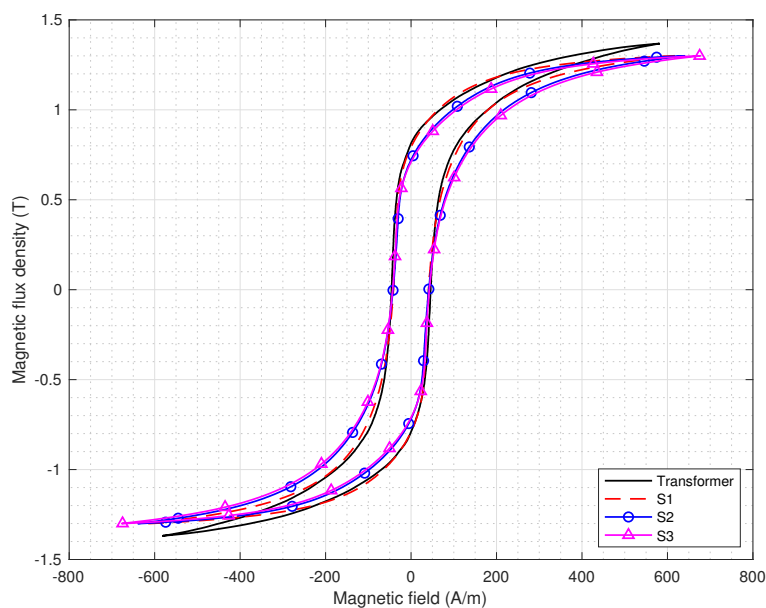


Fig. 11. Comparison between transformer and SST hysteresis loops.

There is a good symmetry between the curves, with a slight difference in the peak values. This difference may appear because, unlike the SST in which the induction is imposed and controlled, in the transformer the observed induction is a consequence of the voltage imposed by the synchronous generator. It is also important to denote that the tests performed on the device take into account the effect of several sheets forming the core, leading to an average magnetic behavior of the sheet pack. On the other hand, in SST, only one sheet is tested at a time, which can lead to differences between the obtained results. In addition, it is important to notice that there will be errors associated to the measurement instruments that can also add uncertainties to the results.

Fig. 12 shows the magnetic losses of the SST test at 1.3 T. For 60 Hz frequency, the average losses



were 2.26 W/kg for hysteresis, 2.01 W/kg for dynamics, and 4.27 W/kg for total. It is important to denote that the test on the SST does not provide separation of dynamic losses, as can be seen from Fig. 12.

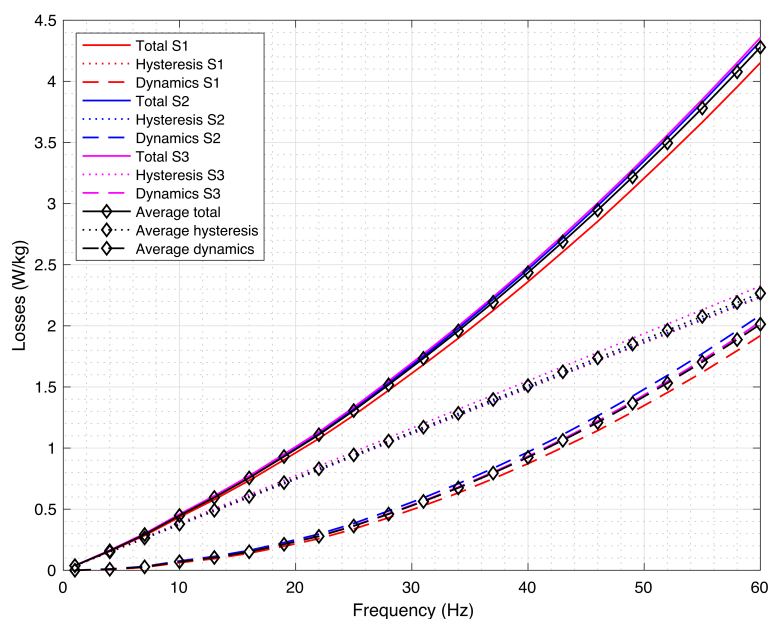


Fig. 12. Magnetic loss measurements realized in SST.

Analyzing the magnetic induction values obtained from the test it is possible to notice that its magnitudes differs: 1.36 T (Fig. 11) from the reduced frequency test, 1.3 T (Fig. 11) from the SST test and 1.15 T (presented at the end of this section) from the no-load test. This difference, when considering the proposed methodology and the SST test is due to the different procedures and equipment used, whereas for the no-load test, the level of magnetic induction at nominal voltage depends on the transformer design.

To enable an accurate quantitative comparison of the results, hysteresis modeling was performed using the experimental BH loop of the transformer and the Jiles-Atherton (JA) model already established in the literature [36]. The JA hysteresis model allows the representation of the BH loops of the material for different levels of magnetic induction. This methodology allows the comparison of the results from the transformer characterization with the results obtained from the SST test and the no-load test at the same induction levels.

The JA parameters were determined with an iterative algorithm [27], using the identification of BH loop points proposed in [37]. An optimization technique was used to fit the calculated curves (H_{calc}) to the experimental ones (H_{exp}). The optimization was performed by minimizing the Mean-Squared Error (MSE) (14) between calculated and experimental data [38].

$$MSE = \frac{1}{p} \sum_{i=1}^p (H_{calc} - H_{exp})^2, \quad (14)$$

where p represents the number of cycle points.

Fig. 13 shows the comparison between the experimental BH loop of the transformer with the parameters determined for JA's model, already optimized, being: $M_s = 1.28 \cdot 10^6$ (A/m); $k = 54.05$ (A/m); $c = 0.1595$; $a = 140.7$ (A/m) and $\alpha' = 4.203 \cdot 10^{-4}$. These parameters adequately represent



the experimental data. The energy density difference between these loops is 2.9%. The simulations presented with the parameters obtained were performed using the inverse model of JA, proposed in [39].

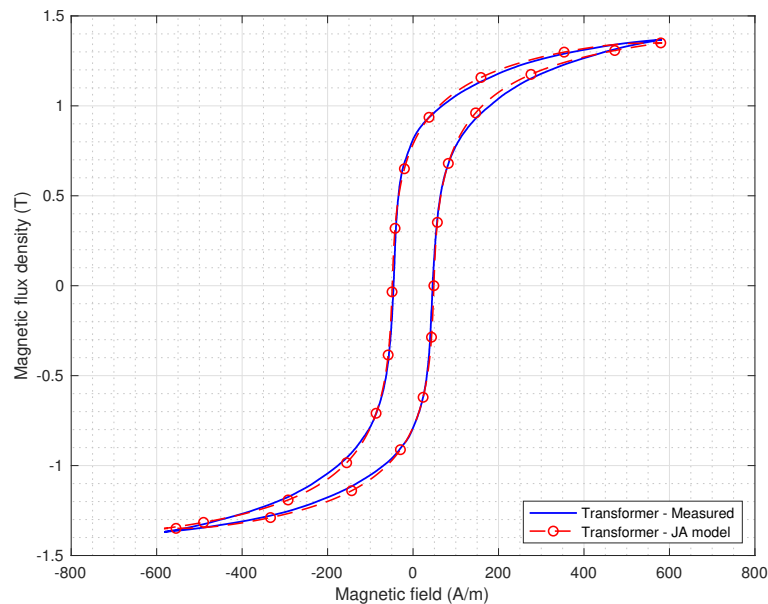


Fig. 13. Comparison between the experimental hysteresis loop of the transformer and the simulated one with JA parameters.

In order to use (2) and (3), σ and $\sqrt{\sigma G V_o S}$ need to be determined. σ was determined by measuring the resistance R_m of the sheets using a four-wire connection, similar to that used in [40]. The measured values are shown in Table IV. It is worth mentioning that for the magnetic characterization in the proposed methodology it is not necessary to determine the resistivity of the sheets. This procedure is performed for validation of the methodology.

TABLE IV. DETERMINATION OF THE CONDUCTIVITY OF THE SHEETS USED IN THE SST

| Sheet | $\overline{R_m}(\Omega)$ | $\overline{\rho}(\Omega \cdot m)$ | $\overline{\sigma}(\Omega \cdot m^{-1})$ | $\overline{\sigma}(\Omega \cdot m^{-1})$ |
|-------|--------------------------|-----------------------------------|--|--|
| S1 | $4.83 \cdot 10^{-3}$ | $4.28 \cdot 10^{-7}$ | $2.34 \cdot 10^6$ | |
| S2 | $4.80 \cdot 10^{-3}$ | $4.24 \cdot 10^{-7}$ | $2.35 \cdot 10^6$ | $2.35 \cdot 10^6$ |
| S3 | $4.83 \cdot 10^{-3}$ | $4.25 \cdot 10^{-7}$ | $2.35 \cdot 10^6$ | |

Once σ is determined, it is possible to calculate $\sqrt{\sigma G V_o S}$ through the separation of dynamic losses:

$$\sqrt{\sigma G V_o S} = \frac{[W_t - (W_h + W_f)] f \cdot m_v}{\frac{1}{T} \int_0^T \left| \frac{dB(t)}{dt} \right|^{\frac{3}{2}} dt} \quad (15)$$

Thus, $\sqrt{\sigma G V_o S}$ is considered to be a constant associated with the excess loss that can be determined by the energy balance. The loss separation consists in obtaining the constants at a single operating point, as a function of the maximum induction of the material [27]. The procedures for the losses separation are:

- 1) Run a test at 5 Hz or lower frequency and determine W_h ;
- 2) Determine W_t by measuring the power dissipated at the rated frequency, keeping the same induction level at which W_h was determined;

- 3) Calculate W_f in the magnetic core (2), at rated frequency and at the same induction level in which W_h was measured;
- 4) Determine $\sqrt{\sigma G V_o S}$ using the energy balance defined in (15).

From the described procedure, applied on the tested sheets, the average value obtained was $\sqrt{\sigma G V_o S} = 0.79$.

Table V shows the comparison between the losses obtained with the hysteresis model parameters for the transformer (JA), calculated with (1), (2) and (3), with those obtained by the SST. The comparison was made using $B = 1.3$ T, being the same induction level as in the SST test. A difference of 4.9% for hysteresis loss, 1.5% for dynamic, and 3.3% in total losses was calculated.

TABLE V. COMPARISON BETWEEN THE LOSSES OBTAINED IN THE SST AND THE SIMULATIONS USING JA

| | Hysteresis (W/kg) | Foucault (W/kg) | Excess (W/kg) | Dynamics (Foucault+Excess) (W/kg) | Total (W/kg) |
|----------------------------------|----------------------|--------------------|------------------|--------------------------------------|-----------------|
| SST measured ¹ | 2.26 | - | - | 2.01 | 4.27 |
| Calculated with JA parameters | 2.15 | 1.28 | 0.70 | 1.98 | 4.13 |

¹ The average loss values shown in Figure 12 were used.

In order to allow the comparison of the core loss shown in the test of Table I, it was necessary to determine the magnetic induction to which the transformer was exposed. From Kirchhoff's voltage law we have

$$v(t) - R_p \cdot i(t) - L_p \cdot \frac{di(t)}{dt} - e(t) = 0, \quad (16)$$

where $v(t)$ is the voltage source, R_p and L_p are, respectively, the resistance and inductance of the primary winding and $i(t)$ is the current. The induced voltage $e(t)$ can be written as

$$e(t) = N_p \cdot \frac{d\phi}{dt}. \quad (17)$$

From (16) and (17) the magnetic induction can be obtained by

$$B(t) = \frac{1}{N_p \cdot S} \int \left(v(t) - R_p \cdot i(t) - L_p \cdot \frac{di(t)}{dt} \right) dt. \quad (18)$$

Solving (18) using the voltage and magnetizing current of Table I, R_p and L_p calculated from the short-circuit test, one can find $B = 1.15$ T.

Table VI shows the comparison between the experimental losses (Table I) with those simulated with the JA parameters. In the calculation, the average density of Table III, $\bar{\sigma}$ of Table IV, $\sqrt{\sigma G V_o S}$ of the separation of dynamic losses, and the core dimensions of Fig. 4 were considered. The result shows a difference, compared to the losses calculated with the JA parameters, of -4% for dynamics losses and -1.8% in total losses.

TABLE VI. COMPARISON BETWEEN NO-LOAD TEST LOSSES AND SIMULATIONS USING JA

| | Hysteresis (W) | Foucault (W) | Excess (W) | Dynamics (Total-Hysteresis) (W) | Total (W) |
|-----------------------|-------------------|-----------------|---------------|------------------------------------|--------------|
| No-load test | | - | - | 24.1 | 54.0 |
| Calculated with JA | 29.9 ¹ | 15.9 | 9.2 | 25.1 | 55.0 |

¹ The values were calculated with JA and B = 1.15 T.

VI. FINAL REMARKS ABOUT THE EXPERIMENTAL PROCEDURE

As stated previously, there is the need for a variable frequency source that endure the rated current of the equipment. It is recommended that the source have a feedback to maintain the symmetry of the BH loops. The quality and reliability of the results obtained depend on the accuracy of the equipment used. Attention must be paid to the determination of the mean magnetic path, because depending on the core type and winding choice for the RFT, the determination of l_{eq} requires a more refined analysis of the magnetic field distribution in the structure. Particular attention must be paid to the transformer's steady state temperature, otherwise the electrical and magnetic characteristics obtained can be significantly changed.

It is important to highlight that in the tests to obtain the losses of magnetic origin, the induced voltage form factor must be kept as close as possible to 1.11. Standards for testing electrical steel agree that a deviation of $\pm 1\%$ from a 1.11 form factor is tolerated [34], [41]. However, it will be necessary to correct the measured loss value if the form factor deviates by more than 1% from the reference value as stated by the standardization guidelines.

VII. CONCLUSION

In this work, a non-invasive methodology for magnetic characterization of transformers and reactors was presented. The methodology was applied to a 2 kVA three-phase dry-type transformer, and the results were compared with experimental data obtained from tests that were carried out on the same material using a Single Sheet Tester device. The proposed methodology allows the characterization of the ferromagnetic material by obtaining the hysteresis loop at low frequency and the separation of hysteresis and dynamic losses.

The comparisons between the hysteresis loops, as well as between the dynamic core losses obtained by the proposed methodology and by the characterization performed with the SST showed agreement with differences lower than 5%. Given this agreement between the field tests and those obtained with the SST in the laboratory, it can be concluded that this methodology is effective for the magnetic characterization of the core, allowing to model the device in different types of transients likely to occur in transformer operation.

Although the characterization has been performed for the three-phase transformer of Fig. 1(e), it can be applied to the different core types shown in Fig. 1, as well as to single-phase transformers and reactors.

ACKNOWLEDGMENTS

This work was supported in part by CNPQ, the Brazilian National Council.

REFERENCES

- [1] X. Liu, C. Yao, S. Liang, J. Wang, and T. Liu, "Measurement of the no-load characteristics of single-phase transformer using an improved low-frequency method," *IEEE Transactions on Industrial Electronics*, vol. 65, no. 5, pp. 4347–4356, 2018.
- [2] Z. Yang, Q. Zhou, X. Wu, and Z. Zhao, "A novel measuring method of interfacial tension of transformer oil combined pso optimized svm and multi frequency ultrasonic technology," *IEEE Access*, vol. 7, pp. 182 624–182 631, 2019.
- [3] J. V. Leite, A. Benabou, N. Sadowski, and M. V. F. da Luz, "Finite element three-phase transformer modeling taking into account a vector hysteresis model," *IEEE Transactions on Magnetics*, vol. 45, no. 3, pp. 1716–1719, 2009.
- [4] A. Rezaei-Zare, R. Iravani, and M. Sanaye-Pasand, "Impacts of transformer core hysteresis formation on stability domain of ferroresonance modes," *IEEE Transactions on Power Delivery*, vol. 24, no. 1, pp. 177–186, 2009.
- [5] N. Chiesa, B. A. Mork, and H. K. Høidalen, "Transformer model for inrush current calculations: Simulations, measurements and sensitivity analysis," *IEEE Transactions on Power Delivery*, vol. 25, no. 4, pp. 2599–2608, 2010.
- [6] S. E. Zirka, D. Albert, Y. I. Moroz, and H. Renner, "Further improvements in topological transformer model covering core saturation," *IEEE Access*, vol. 10, pp. 64 018–64 027, 2022.
- [7] A. Rezaei-Zare, R. Iravani, M. Sanaye-Pasand, H. Mohseni, and S. Farhangi, "An accurate hysteresis model for ferroresonance analysis of a transformer," *IEEE Transactions on Power Delivery*, vol. 23, no. 3, pp. 1448–1456, 2008.
- [8] J. Martinez, R. Walling, B. Mork, J. Martin-Arnedo, and D. Durbak, "Parameter determination for modeling system transients-part iii: Transformers," *IEEE Transactions on Power Delivery*, vol. 20, no. 3, pp. 2051–2062, 2005.
- [9] A. Rezaei-Zare, M. Sanaye-Pasand, H. Mohseni, S. Farhangi, and R. Iravani, "Analysis of ferroresonance modes in power transformers using preisach-type hysteretic magnetizing inductance," *IEEE Transactions on Power Delivery*, vol. 22, no. 2, pp. 919–929, 2007.
- [10] J. Lacerda Ribas, E. M. Lourenço, J. Leite, and N. Batistela, "Modeling ferroresonance phenomena with a flux-current jiles-atherton hysteresis approach," *IEEE Transactions on Magnetics*, vol. 49, no. 5, pp. 1797–1800, 2013.
- [11] M. Shafieipour, W. Ziomek, R. P. Jayasinghe, J. C. G. Alonso, and A. M. Gole, "Application of duality-based equivalent circuits for modeling multilimb transformers using alternative input parameters," *IEEE Access*, vol. 8, pp. 153 353–153 363, 2020.
- [12] F. De Leon and A. Semlyen, "A simple representation of dynamic hysteresis losses in power transformers," *IEEE Transactions on Power Delivery*, vol. 10, no. 1, pp. 315–321, 1995.
- [13] E. Cardelli, E. Della Torre, V. Esposito, and A. Faba, "Theoretical considerations of magnetic hysteresis and transformer inrush current," *IEEE Transactions on Magnetics*, vol. 45, no. 11, pp. 5247–5250, 2009.
- [14] C. Huo, S. Wu, Y. Yang, C. Liu, and Y. Wang, "Residual flux density measurement method of single-phase transformer core based on time constant," *IEEE Access*, vol. 8, pp. 171 479–171 488, 2020.
- [15] Y. Pan, X. Yin, Z. Zhang, B. Liu, M. Wang, and X. Yin, "Three-phase transformer inrush current reduction strategy based on prefluxing and controlled switching," *IEEE Access*, vol. 9, pp. 38 961–38 978, 2021.
- [16] A. D. Theocharis, J. Miliaris-Argitis, and T. Zacharias, "Single-phase transformer model including magnetic hysteresis and eddy currents," *Electrical Engineering*, vol. 90, no. 3, pp. 229–241, May. 2007.
- [17] ———, "Three-phase transformer model including magnetic hysteresis and eddy currents effects," *IEEE Transactions on Power Delivery*, vol. 24, no. 3, pp. 1284–1294, July 2009.
- [18] P. S. Moses, M. A. S. Masoum, and H. A. Toliyat, "Dynamic modeling of three-phase asymmetric power transformers with magnetic hysteresis: No-load and inrush conditions," *IEEE Transactions on Energy Conversion*, vol. 25, no. 4, pp. 1040–1047, 2010.
- [19] A. Gaudreau, P. Picher, L. Bolduc, and A. Coutu, "No-load losses in transformer under overexcitation/inrush-current conditions: tests and a new model," *IEEE Transactions on Power Delivery*, vol. 17, no. 4, pp. 1009–1017, 2002.
- [20] H. Lamba, M. Grinfeld, S. McKee, and R. Simpson, "Subharmonic ferroresonance in an lcr circuit with hysteresis," *IEEE Transactions on Magnetics*, vol. 33, no. 4, pp. 2495–2500, 1997.
- [21] H. Li, L. Wang, J. Li, and J. Zhang, "An improved loss-separation method for transformer core loss calculation and its experimental verification," *IEEE Access*, vol. 8, pp. 204 847–204 854, 2020.
- [22] G. M. R. Negri, N. Sadowski, N. J. Batistela, J. V. Leite, and J. P. A. Bastos, "Magnetic aging effect losses on electrical steels," *IEEE Transactions on Magnetics*, vol. 52, no. 5, pp. 1–4, 2016.
- [23] R. M. D. Vecchio, B. Poulin, P. T. Feghali, D. M. Shah, and R. Ahuja, *Transformer design principles*, third edition ed. CRC Press, 2018.
- [24] G. Novak, J. Kokošar, A. Nagode, and D. S. Petrovič, "Core-loss prediction for non-oriented electrical steels based on the steinmetz equation using fixed coefficients with a wide frequency range of validity," *IEEE Transactions on Magnetics*, vol. 51, no. 4, pp. 1–7, 2015.

- [25] O. Osemwinyen, A. Hemeida, F. Martin, I. T. Gürbüz, P. S. Ghahfarokhi, and A. Belahcen, “Determination of core losses using an inverse modeling technique,” *IEEE Access*, vol. 10, pp. 29 224–29 232, 2022.
- [26] J. Bastos, *Eletromagnetismo para engenharia: estática e quase-estática*, 3rd ed. Editora UFSC, 2012.
- [27] N. J. Batistela, “Caracterização e modelagem eletromagnética de lâminas de aço ao silício,” Ph.D. dissertation, Universidade Federal de Santa Catarina, Programa de Pós-graduação em Engenharia Elétrica, Florianópolis, 2001.
- [28] G. Bertotti, “General properties of power losses in soft ferromagnetic materials,” *IEEE Transactions on Magnetics*, vol. 24, no. 1, pp. 621–630, 1988.
- [29] I. S. C57.123-2019, “Ieee guide for transformer loss measurement,” *IEEE Std C57.123-2019 (Revision of IEEE Std C57.123-2010)*, pp. 1–55, 2020.
- [30] I. S. C57.12.91-1995, “Ieee standard test code for dry-type distribution and power transformers,” *IEEE Std C57.12.91-1995*, pp. 1–88, 1996.
- [31] E. So, R. Arseneau, and E. Hanique, “No-load loss measurements of power transformers under distorted supply voltage waveform conditions,” *IEEE Transactions on Instrumentation and Measurement*, vol. 52, no. 2, pp. 429–432, 2003.
- [32] I. E. Commissio, “Power transformers - part 11: Dry-type transformers,” *IEC 60076-11:2018*, pp. 1–124, 2018.
- [33] S. K. S.V. Kulkarni, *Transformer Engineering: Design, Technology, and Diagnostics, Second Edition*, 2nd ed. CRC Press, 2012.
- [34] A. B. de Normas Técnicas, “Produtos laminados planos de aço para fins elétricos - verificação das propriedades,” *NBR 5161*, pp. 1–35, 1977.
- [35] B. Measurements, “Measuring unit mpg 200 data manual,” Brockhaus, Lüdenscheid, Germany, technical report, 2000.
- [36] D. Jiles and D. Atherton, “Theory of ferromagnetic hysteresis,” *Journal of Magnetism and Magnetic Materials*, vol. 61, no. 1, pp. 48–60, 1986. [Online]. Available: <https://www.sciencedirect.com/science/article/pii/0304885386900661>
- [37] D. Jiles, J. Thielke, and M. Devine, “Numerical determination of hysteresis parameters for the modeling of magnetic properties using the theory of ferromagnetic hysteresis,” *IEEE Transactions on Magnetics*, vol. 28, no. 1, pp. 27–35, 1992.
- [38] J. V. Leite, “Análise de modelos diferenciais de histerese magnética considerando laços menores de indução,” Master’s thesis, Universidade Federal de Santa Catarina, Programa de Pós-graduação em Engenharia Elétrica, Florianópolis, 2002.
- [39] N. Sadowski, N. Batistela, J. Bastos, and M. Lajoie-Mazenc, “An inverse Jiles-Atherton model to take into account hysteresis in time-stepping finite-element calculations,” *IEEE Transactions on Magnetics*, vol. 38, no. 2, pp. 797–800, 2002.
- [40] B. J. Mailhé, “Characterization and modelling of the magnetic behaviour of electrical steel under mechanical stress,” Ph.D. dissertation, Universidade Federal de Santa Catarina, Programa de Pós-graduação em Engenharia Elétrica, Florianópolis, 2018.
- [41] J. S. Association, “Test methods for electrical steel strip and sheet - part 1: Methods of measurement of the magnetic properties of electrical steel strip and sheet by means of an epstein frame,” *JIS C 2550-1*, pp. 1–37, 2000.